Cloning and Functional Characterization of Two Calmodulin Genes During Larval Development in the Parasitic Flatworm Schistosoma mansoni

Authors: Taft, Andrew S., and Yoshino, Timothy P.

Source: Journal of Parasitology, 97(1) : 72-81

Published By: American Society of Parasitologists

URL: https://doi.org/10.1645/GE-2586.1

J. Parasitol., 97(1), 2011, pp. 72–81

CLONING AND FUNCTIONAL CHARACTERIZATION OF TWO CALMODULIN GENES DURING LARVAL DEVELOPMENT IN THE PARASITIC FLATWORM *SCHISTOSOMA MANSONI*

Andrew S. Taft and Timothy P. Yoshino

Department of Pathobiological Sciences, School of Veterinary Medicine, University of Wisconsin, Madison, Wisconsin 53706. *e-mail: yoshinot@svm.vetmed.wisc.edu*

ABSTRACT: Schistosomiasis is endemic in over 70 countries, in which more than 200 million people are infected with the various schistosome species. Understanding the physiological processes underlying key developmental events could be useful in developing novel chemotherapeutic reagents or infection intervention strategies. Calmodulin is a small, calcium-sensing protein found in all eukaryotes and, although the protein has been previously identified in various *Schistosoma mansoni* stages and implicated in egg hatching and miracidia transformation, few molecular and functional data are available for this essential protein. Herein, we report the molecular cloning, expression, and functional characterization of calmodulin in the miracidia and primary sporocyst stages of *S. mansoni*. Two transcripts, SmCaM1 and SmCaM2, were cloned and sequenced, and a recombinant SmCaM1 protein was expressed in *Escherichia coli* and used to generate anti-CaM antibodies. The 2 protein sequences were highly conserved when compared to other model organisms. The alignment of the predicted proteins of both SmCaM1 and SmCaM2 exhibited 99% identity to each other and 97–98% identity with mammalian calmodulins. Analysis of steady-state transcript abundance indicate that the 2 calmodulin transcripts differ in their stage-associated expression patterns, although the CaM protein isotype appears to be constitutively expressed during early larval development. Application of RNAi to larval parasites results in a ''stunted growth'' phenotype in sporocysts with 30 and 35% reduction in transcript abundance for SmCaM1 and SmCaM2, respectively, and a corresponding 35% reduction in protein level after incubation in double-stranded RNA. Differential expression of CaM transcripts during early larval development and a growth defect-inducing effect associated with partial transcript and protein inhibition as a result of RNAi suggest a potentially important role of calmodulin during early larval development.

Schistosomiasis is a debilitating disease caused by several parasitic species of *Schistosoma*. Approximately 200 million individuals are infected with schistosomes, with an estimated 779 million people in over 70 countries worldwide at risk of infection (Steinmann et al., 2006; King, 2007). Patients infected with various species of schistosomes display spleno- and hepatomegaly, anemia, diarrhea, and increased risk for bladder cancer; in children, the disease results in impaired cognitive development and slow physical growth (www.cartercenter.org/health/schistosomiasis/index.html). The most commonly used chemotherapeutic, praziquantel, is a relatively inexpensive drug with high efficacy in reducing worm burden, thus alleviating the morbidity associated with infection by all human schistosome species (Doenhoff et al., 2008). However, recently there have been reports of reduced sensitivity to praziquantel in *Schistosoma mansoni* strains isolated from infected individuals following multiple rounds of treatment (Melman et al., 2009). Developing resistance to the drug illustrates not only the need to identify new targets for chemotherapeutic intervention, but also the requirement to seek novel approaches for disrupting parasite development whether in the human or molluscan hosts.

The life cycle of *S. mansoni* is complex, involving many physiological, transcriptional, biochemical, and morphological changes as it cycles between its mammalian and snail hosts. Intramolluscan development is initiated when freshly hatched, free-swimming miracidia seek out and actively penetrate the snail's mantle epithelium, where they then transform into, and begin developing to, the primary sporocysts, the first intramolluscan parasitic stage. Although several studies have profiled gene expression changes associated with this miracidium-to-sporocyst developmental transition with the use of microarray technology (Vermeire et al., 2006; Jolly et al., 2007; Fitzpatrick et al., 2009) and serial analysis of gene expression (Taft et al., 2009), very few have functionally characterized the role of specific transformation-associated genes during this phase of early larval development.

Calmodulin and calcium signaling play essential roles during certain stages of *S. mansoni* development. For example, selective calmodulin inhibitors are known to disrupt egg hatching or cause miracidia to become vesiculated and die without undergoing transformation to the sporocyst stage (Katsumata et al., 1988, 1989; Kawamoto et al., 1989). Calcium mobilization also plays a role in the cercarial penetration processes, possibly by calcium regulation of protease activities during infection (Lewert et al., 1966; Fusco et al., 1991). Levels of calcium in the penetration glands of cercariae exceed 8–10 M and, at these high levels, the proteases within these glands are inactive. However, upon release of these enzymes to the external environment, the proteolytic activity functionally resumes (Dresden and Edlin, 1974). Calcium signaling is also involved in the excystment of *Paragonimus ohirai* metacercariae, possibly indicating conserved signals for larval development in multiple trematode species (Ikeda, 2001, 2004, 2006). However, the specific role of calmodulin in these Ca-dependent processes has not been elucidated.

Calcium ions are important second messengers that are crucial for many biological functions, including muscle contraction, metabolism, and cell motility, i.e., ciliary and flagellar motion (Salathe, 2007). Fluctuations in intracellular calcium levels are transduced by a variety of calcium sensors, although calmodulin, a small calcium-binding protein that is found in all eukaryotic animals, represents one of the primary, and best studied, calcium sensors. Mammalian calmodulin (CaM) is typically a protein of 16 kDa, comprised of 2 globular domains connected by a flexible alpha helix hinge. Each of these clusters contains 2 Ca^{+2} binding EF-hand domains, making the molecule very sensitive to even small fluctuations in Ca^{+2} concentrations. Although CaM has no intrinsic catalytic activity, it functions as a calcium sensor and signal transducer by undergoing a conformational change when bound to calcium and, then, in turn, serving to activate specific

Received 7 July 2010; revised 26 August 2010; accepted 30 August 2010.
DOI: 10.1645/GE-2586.1

enzymes involved in such diverse functions as cyclic nucleotide synthesis and metabolism, phosphorylation/dephosphorylation of protein kinases and phosphatases, gene transcription, and Ca^{+2} transport (Cohen and Klee, 1988). The number of specific proteins regulated by CaM is large and represents diverse families; for example, using mRNA-display, Shen et al. (2008) identified 56 Ca^{2+}/calmodulin binding proteins in *Caenorhabditis elegans* that included CaM-dependent kinases, myosin family members, heat shock proteins, protein phosphatases, and phosphodiesterases.

Although calmodulin has been widely studied and well characterized in many organisms, there are very few data on the role of CaM in schistosome biology. A number of calcium-binding ''CaM-like'' proteins have been identified in *S. mansoni* and *Schistosoma japonicum*, including Sme16, Sm20, and SjCa8, but none of these has a ''classical'' CaM sequence or structure (Havercroft et al., 1990; Moser et al., 1992; Hu et al., 2008). The presence of CaM-like proteins recently was demonstrated in larval excretory–secretory culture supernatants of sporocysts having undergone in vitro transformation (Wu et al., 2009), cercariae undergoing in vitro transformation to the schistosomula stage (Knudsen et al., 2005), and in adult *S. mansoni* using immunoblot analysis (Thompson et al., 1986). Although this evidence supports the presence of CaM in schistosomes, there is still little known regarding the molecular structure, expression, localization, and specific function of these Ca-binding proteins within larval schistosomes, especially during miracidium-to-primary sporocyst transformation and subsequent early larval development. Because of earlier evidence suggesting a putative role for CaM in egg hatching and miracidium transformation, we sought to further characterize this important protein in larval *S. mansoni* and investigate its role in early larval schistosome development.

MATERIALS AND METHODS

Parasite isolation and short-term culture

Freshly hatched *S. mansoni* NMRI -strain miracidia were isolated from eggs recovered from the livers of Swiss-Webster mice, 7–8 wk postinfection (PI) as described by Yoshino and Laursen (1995). Miracidia were concentrated in 15-ml tubes by placing them on ice for 15 min, followed by centrifuging the tubes at 4 C for 15 min at 500 *g*, resuspending pelleted larvae in fresh ice-cold artificial pond water (APW; Nolan and Carriker, 1946), and centrifuging again at 4 C for 15 min at 500 *g*. The miracidia were either used immediately for further studies or resuspended in Chernin's balanced salt solution (CBSS; Chernin, 1963) containing 1 mg/ml of glucose and trehalose, penicillin G (0.06 mg/ml), and streptomycin sulfate (0.05 mg/ml [CBSS+] for axenic cultivation and transformation to primary sporocysts. Sporocysts were maintained in CBSS+ at 26 C under normoxic conditions.

cDNA cloning and sequencing of 2 calmodulin transcripts

Total RNA was isolated from parasites with the use of the TRIzol reagent (Invitrogen, Carlsbad, California) following the manufacturer's protocol. Total RNA was DNAse treated with the use of the TURBO DNase kit (Ambion, Austin, Texas) and quantified with the use of a Nanodrop ND-1000 spectrophotometer (NanoDrop Technologies, Wilmington, Delaware). Two micrograms of a 1:1 mix of miracidia and 6-day sporocyst total RNA was used to synthesize 3′ and 5′ RACE templates with the GeneRacer kit (Invitrogen), as per the manufacturer's protocol. The 5′ cDNA ends were then PCR amplified with the use of the following transcript-specific primers SmCaM1 (5′-CGACTCAACACGCCAATCAC) and SmCaM2 (5′-AGACGAAAAGAATGAACGTGAACA), along with the GeneRacer 5′ outer primer. Partial CaM transcript-specific sequences were obtained from SchistoDB (Zerlotini et al., 2009). PCR reaction products were gel purified and subjected to a second round of amplification with the same transcript specific primers and the GeneRacer 5′ nested primer. Amplicons were again gel purified and cloned into the TOPO-TA Cloning Kit (Invitrogen) as per manufacturer's instructions. Positive clones were sequenced with vector-specific primers with the use of BigDye chemistry (Applied Biosystems, Foster City, California) in conjunction with the University of Wisconsin Biotechnology DNA Sequencing Center. The 3′ cDNA sequences were amplified and cloned in the same way, albeit using 3′ RACE templates with the GeneRacer 3′ outer primer and nested primer, along with the following transcript-specific primers: SmCaM1 (5′-TTGAGCAAATGAATGTCTGTAAAGC-3′) and SmCaM2 5′-CCTCGCTTTACCATCTCACGA-3′). Resulting sequences were vector trimmed and aligned with the use of the ContigExpress program from the VectorNTI software suite (Invitrogen). BlastX searches of the NCBI protein database confirmed sequence identity.

Identification of genomic structure

Genomic DNA was isolated from freshly hatched miracidia with the use of the DNAeasy Tissue Kit (Qiagen, Valencia, California) as per manufacturer's instructions, and DNA was quantified with the use of the NanoDrop ND-1000 as previously described. Polymerase chain reaction (PCR) was performed with 50 ng of total DNA with the use of the common forward primer (5′-ATGTAATGACTAACTTGGGCGAAA-3′) and the SmCaM1 transcript-specific reverse primer (5′-TGGCACAGTAACAAACTCAATCATTGGA-3′) or the SmCaM2 specific-reverse primer (5′-AGTGTGATGAGAATGTTTAGTTCTGATGTA-3′). PCR reactions were run out on a 1.2% agarose gel and the resulting bands were gel purified and sequenced.

Real-time quantitative PCR (qPCR) of calmodulin mRNA transcripts

SmCaM1 and SmCaM2 steady-state transcript levels were quantified in miracidia and in 1-, 3-, and 8-day in vitro cultured sporocysts with the use of an ABI 7500 Real-Time PCR System (Applied Biosystems). Complementary DNA (cDNA) was synthesized with the use of the Superscript III cDNA synthesis kit (Invitrogen) and the supplied dT primer from 1 μg of DNase-treated total RNA from miracidia and 1-, 3- and 8-day in vitro cultured sporocysts. qPCR reactions were performed on an ABI 7500 Real Time PCR system (Applied Biosystems) using 600 nM of each gene-specific primer with SYBR Green 2X PCR master mix (Applied Biosystems) and glyceraldehyde-3-phosphate dehydrogenase (GAPDH) serving as a nonchanging loading control. A dissociation curve was performed at the end of each qPCR run to ensure amplification specificity. qPCR primers were designed with the use of Primer Express 3.0 (Applied Biosystems) using the following default parameters: amplicon length of 50–150 base pairs (bp), a T_m of 68–70 C, and a % GC of 30–80%. Primers used for qPCR are as follows: SmCaM1-forward (5′-TTGAGCAAATGAATGTCTGTAAAGC-3′), SmCaM1-reverse (5′-CGACTCAACACGCCAATCAC-3′), SmCaM2-forward (5′-CCTCGCTTTACCATCTCACGA-3′), SmCaM2-reverse (5′-AGACGAAAAGAATGAACGTGAACA-3′), GAPDH-forward (5′-TCGTTGAGTCTACTGGAGTCTTTACG-3′) and GAPDH-reverse (5′-AATATGAGCCTGAGCTTTATCAATGG-3′). Each experiment consisted of 3 separate biological replicates, each of which was comprises 3 technical replicates. Standard qPCR controls were performed, including a no-template control and a no-reverse-transcriptase control in the reverse transcription reaction. Relative transcript abundance was calculated with the use of the delta-delta Ct method (Livak and Schmittgen, 2001).

Recombinant calmodulin expression, purification, and antibody production

The full-length open reading frame (ORF) of SmCaM1 was PCR amplified from pooled miracidia and 2-day in vitro cultured sporocyst cDNA with the use of the following primers: forward 5′-GACGACGACAAGATGGCCGACCAATTAACAGAGGAACAG-3′ and reverse 5′-GAGGAGAAGCCCGGTTACTTTGTCGTCATCATTGTAACAAATTCTTCATA-3′. The amplified product was gel purified, cloned into the Novagen pET-46 Ek/LIC protein expression vector (EMD4Biosciences, San Diego, California) as per the manufacturer's instructions and transformed into the NovaBlue *E. coli* cell line (EMD4Biosciences). Putative clones were sequenced using pET-46-specific primers to ensure proper sequence and then subcloned into the BL21 (DE3) protein

expression cell line. A 250-ml bacterial culture was grown in a shaking incubator until the OD_{600} reached 2.0, after which the cells were centrifuged, resuspended in 20 ml binding buffer (20 mM sodium phosphate, 0.5 M NaCl, 15 mM imidazole, pH 7.4) and 200 µl protease inhibitor cocktail (Sigma-Aldrich, St. Louis, Missouri), sonicated and then centrifuged at 8,000 *g* for 15 min at 4 C. The recombinant protein was purified using a HisTrap HP Nickel affinity column (GE Healthcare Bio-Sciences Corp., Piscataway, New Jersey), run on a 12.5% SDS-PAGE gel and stained with Coomassie blue to ensure proper size and purity, and finally dialyzed against mammalian PBS for antibody production. Five milliliters of preimmune serum were taken from a single rabbit prior to immunization, followed by injection of 0.5 mg of purified SmCaM1 in Freund's complete adjuvant on day 0, and subsequent boosts with 0.25 mg of protein in Freund's incomplete adjuvant on days 21 and 42. Hyperimmune serum samples were obtained on days 42, 56, and 70.

Immunocytochemical localization of calmodulin in miracidia and sporocysts

Miracidia and 3-day in vitro cultured sporocysts were simultaneously fixed and permeabilized in a mixture of 4% paraformaldehyde and 1% Triton X-100 in snail-buffered PBS (sPBS, pH 7.4; Yoshino, 1981) at 4 C overnight with constant rotation (Barnstead Labquake rotator, Thermo Fisher Scientific, Waltham, Massachusetts). The fixed specimens were washed 5× for 10 min in sPBS at RT, blocked overnight in blocking buffer (5% normal goat serum in sPBS) at 4 C under constant rotation, and washed again with sPBS 5× for 10 min at RT. After washing fixed larvae were incubated in a 1:1,000 dilution of anti-SmCaM in blocking buffer overnight at 4 C under constant rotation, washed again with sPBS 5× for 10 min at RT and then incubated in 50 µg/ml Hoechst 33258 dye (Invitrogen, Eugene, Oregon), 7.5 U/ml Alexa Fluor®546-conjugated phalloidin (Invitrogen), and 4 µg/ml Alexa Fluor®488-conjugated goat anti-rabbit secondary antibody (Invitrogen). Finally, parasites were washed (5× for 10 min in sPBS), and mounted on glass coverslips with the use of Vectashield mounting medium (Vector Laboratories, Burlingame, California). Images were collected with the use of a Nikon AR1 high-speed spectral confocal microscopy system (Nikon Instruments, Inc., Melville, New York) and processed with the Nikon NIS-Elements software package.

Western blotting and calcium binding properties of calmodulin

Protein abundance levels of calmodulin were assessed by standard Western blotting techniques (Sambrook, 1989). Groups of parasites (miracidia, 1-, 3-, and 8-day) were homogenized by sonication in PARIS buffer (Ambion) and total protein levels in each sample were quantified with the use of a bicinchoninic acid (BCA) assay (Pierce, Rockford, Illinois). Two micrograms of each sample were mixed with 5× SDS/PAGE loading buffer and separated on a 10% SDS-polyacrylamide gel with the use of a Mini Protean II apparatus (Bio-Rad, Hercules, California). Proteins were transferred to a nitrocellulose membrane with the use of a Hoefer TE semidry transfer apparatus (Amersham Biosciences, Piscataway, New Jersey). The membrane was blocked overnight at 4 C in a Tris-buffered saline (TBS: 20 mM Tris/150 mM NaCl, pH 7.5) blocking buffer containing 5% powdered milk and 0.1% Tween-20. The membrane was cut horizontally and the top half was incubated in a mouse anti-alpha tubulin antibody in blocking buffer (serving as loading control, 1:1,000 dilution; Upstate Biotechnology Inc., Lake Placid, New York), and the bottom half was incubated in a 1:5,000 dilution of anti-SmCaM in blocking buffer for 2 hr at room temperature (RT). The membrane was washed 3× for 20 min with TBS with 0.1% Tween-20 (TBST), then incubated in a 1:10,000 dilution of alkaline phosphatase (AP)-conjugated anti-rabbit IgG antibody in blocking buffer, followed again by washing 3× for 20 min in TBST at RT. Immunoreactivity was detected with the use of 5-bromo-4-chloro-3-indolyl phosphate (BCIP) and nitro-blue tetrazolium (NBT) diluted in AP buffer (0.1 M Tris, 0.1 M NaCl, 0.05 M $MgCl_2$, pH 9.5). To investigate the characteristic calcium binding properties of recombinant SmCaM, 1 µg of purified protein was added to gel loading buffer containing 1 mM EDTA or 1 mM $CaCl_2$, followed by separation on a 12.5% nondenaturing polyacrylamide gel (lacking SDS) in which 1 mM EDTA or 1 mM $CaCl_2$ was incorporated into the gel. Proteins were visualized by staining with Coomassie blue.

Trifluoperazine treatment of miracidia

To determine if CaM might be involved in miracidium transformation, trifluoperazine, a known antagonist of CaM (Sheterline, 1980), was used in a modified larval transformation assay (Taft et al., 2010). Approximately 150 freshly hatched miracidia in 100 µl complete BGE medium (cBGE; Hansen et al., 1974) were added to individual wells of a 96-well plate. Trifluoperazine in 2% DMSO, or DMSO only (carrier control), was added to each well at final compound concentrations of 10, 5, 2, and 0.5 µM. Miracidia were then incubated at 26 C for 18 hr, at which time they were examined with the use of a light microscope and scored as nontransformed if ciliated plates were intact and larvae were still swimming or transforming/transformed if they assumed a ''rounded'' morphology and were in the process of shedding epidermal plates or were completely transformed, i.e., sporocyst tegument was fully formed with no ciliated plates remaining attached. Following larval evaluation, parasites were fixed in 4% paraformaldehyde and the total numbers of parasites per well were quantified. Tests for each compound concentration were performed in triplicate on 2 separate occasions (2 independent biological replicates).

Effects of calmodulin double-stranded (ds)RNA treatment on larval schistosomes

Double-stranded (ds) RNA templates were amplified from *S. mansoni* cDNA with the use of the following T7-tagged primers (corresponding to the ORF of both SmCaM1 and SmCaM2): forward (5′-GAGGA-GAAGCCCGGTTACTTTGTCGTCATCATTGTAACAAATTCTTC-ATA-3′) and reverse (5′-TAATACGACTCACTATAGGGCTTCACG-TATCATTTCATCGACCT). The PCR products were gel purified and sequenced to ensure proper identity; 200 ng of purified DNA template were used in a dsRNA synthesis reaction with the use of the T7 Ribomax kit (Promega, Madison, Wisconsin). Green fluorescent protein (GFP) dsRNA template was generated as described previously (Mourao et al., 2009) and used as a nonspecific dsRNA control. All dsRNA reaction mixtures were DNase treated to remove the DNA template and purified using phenol:chloroform as per the manufacturer's instructions. dsRNA was run on an agarose gel to ensure integrity and proper size and then quantified using a Nanodrop ND-1000 spectrophotometer (NanoDrop Technologies, Wilmington, Delaware). Treatment of parasites with dsRNA was performed by placing ~5,000 freshly hatched miracidia into wells of a 24-well plate containing 100 nM dsCaM or dsGFP in CBSS+ and incubated under normoxic conditions at 26 C. On days 3 and 5, approximately half of the CBSS+ medium was removed and replenished with fresh medium containing 100 nM dsRNA. After 7 days of dsRNA treatment, parasites were washed with CBSS+ and the parasites were used for total RNA isolation, protein extraction, or fixed for immunocytochemistry (as described below). Three separate biological replicates were performed.

RESULTS

Identification, cloning, and sequencing of 2 schistosome calmodulin transcripts

Previous studies using serial analysis of gene expression (SAGE) identified an expressed sequence tags (EST) cluster (Sm03962) with high homology to calmodulin from other organisms (Taft et al., 2009). A blast search of the *S. mansoni* genome (http://old.genedb.org/) using Sm03962 as the query identified another EST cluster (Sm07755) that was nearly identical to Sm03962, but coded for another putative calmodulin. Due to the high identity of the 2 EST sequences and possible sequencing and/or clustering errors in the reported transcript segments, we performed 5′ and 3′ RACE using primers designed to the nonidentical regions to determine the full coding sequences of the 2 transcripts. The complete cDNA sequences of SmCaM1 and SmCaM2 were obtained by 5′ and 3′ RACE with the use of primers from the 3′ UTR that do not cross react with the 2 separate transcripts (data not shown). The full-length cDNA for

SmCaM1 (GenBank™ accession no. HQ163799) is 812 bp and SmCaM2 SmCaM1 (GenBank™ accession no. HQ163800) is 1,116 bp, and both have ORFs of 450 bp encoding proteins of 149 amino acids with predicted molecular weights of 16.8 kDa. Sequence analysis of the 5′ UTRs indicates that SmCaM1 has an additional 51 bp of sequence at the 5′ end compared to SmCaM2. The 3′ UTRs diverge 22 bp before the stop codon and are 24% identical to each other. Protein alignment of SmCaM1 and SmCaM2 demonstrate only 2 amino acid differences between them and both are located at the C-terminus (-KMMTAK vs. -TMMTTK, respectively) (Fig. 1A). Moreover alignment of the 2 *S. mansoni* CaM proteins with other CaMs (Fig. 1B) show that both predicted proteins share 98% or greater identity with other CaMs from mammals, insects, and flatworms, demonstrating that CaMs are highly conserved proteins found throughout the animal kingdom. SmCaM1 differs from human calmodulin by 3 residues (F100Y, D120E, and K144Q), whereas SmCaM2 differs by 4 residues (F100Y, D120E, T144Q, and T148A). BLAST analysis of the *S. mansoni* genome (http://www.genedb.org/genedb/smansoni) of the 2 predicted cDNAs locate SmCaM1 on Smp_scaff000053 (of length 818,357 bp), whereas there are no genomic data for SmCaM2. From physical mapping by Criscione et al. (2009), it is known that Smp_scaff000053 is found at 233.7 centimorgans on the Z (sex) chromosome.

Genomic organization of CaM genes

PCR was performed with genomic DNA to identify intron/exon boundaries and to determine if the 2 CaM transcripts were possibly derived from alternate splicing. A primer designed from the ORF, identical in both transcripts, and a transcript unique to SmCaM1 or SmCaM2 were used for PCR. Results indicate that the SmCaM2 gene contains no introns, whereas there are 4 predicted introns in SmCaM1.

Transcript abundance analysis of miracidia and in vitro developing sporocysts

Quantitative real-time RT-PCR (qPCR) was performed on miracidia and in vitro developing primary sporocysts to identify changes in transcript abundance during larval development. Three independent biological replicates from miracidia and 1-, 3-, and 8-day in vitro cultured sporocysts were used. Compared to the steady-state SmCaM1 transcript levels in miracidia, abundance of SmCaM1 mRNA in 1-day cultured sporocysts decrease significantly, but then gradually increased in 3- and 8- day sporocysts (Fig. 2A), whereas SmCaM2 transcript levels increased in 1- and 3-day sporocysts followed by a decrease in larval levels by 8-day sporocysts in culture (Fig. 2B).

Production of recombinant SmCaM protein and protein expression during larval development

SmCaM1 was expressed as a soluble protein in *E. coli* and purified from induced bacterial cell culture supernatants with the use of the N-terminus hexa-histidine tag. The purified protein did not contain any visible impurities in a Coomassie brilliant blue stained protein gel (Fig. 3A). Western blot analyses of miracidia and in vitro developing sporocysts demonstrate no discernible differences in calmodulin protein levels between miracidia, 1-, 3-, and 8-day in vitro cultured sporocysts (Fig. 3B). Because of the 99% identity of SmCaM1 and SmCaM2, we assume that our polyclonal antibody reacts with similar efficiency to both *S. mansoni* calmodulin proteins. A second, higher-molecular-weight band can be observed in the Western blot and may be due to posttranslational modification of calmodulin.

Tissue localization of CaM in miracidia and 3-day sporocysts with the use of confocal microscopy

To determine the tissue distribution of calmodulin in miracidia and in vitro cultured sporocysts, we incubated fixed and permeabilized parasites with the polyclonal anti-SmCaM followed by incubation with Alexa-fluor 488 secondary antibody and visualized the reactivity using confocal microscopy. Parasites were co-incubated with Hoechst 33258 and Alexa Fluor®546-conjugated phalloidin to assist in tissue identification and localization of immunoreactive SmCaM. In the miracidia, intense anti-SmCaM reactivity was observed in the cilia, epidermal plates and multiciliated sensory papillae (Fig. 4A). In 3-day in vitro cultured sporocysts, immunoreactivity was confined primarily to the tegumental layer (Fig. 4B).

Functional analysis of *S. mansoni* calmodulin

Calcium binding function: To demonstrate the calcium binding properties of SmCaM1, the recombinant protein was separated on native (nonreducing) polyacrylamide gels containing 1 mM EDTA or 1 mM $CaCl_2$. SmCaM1 demonstrated increased electrophoretic mobility in the presence of EDTA in the gel, compared to $CaCl_2$, strongly supporting a Ca ion-binding function for recombinant SmCaM1 (Fig. 5).

Effects of the calmodulin antagonist, trifluoperazine, on miracidium transformation: The commonly used and well-characterized calmodulin antagonist, trifluoperazine, inhibits the in vitro transformation of miracidia in a dose-dependent manner. As shown in Figure 8, after 18 hr of culture in 2% DMSO, 80% (±3%) of the miracidia were transformed or in the transformation process, whereas miracidia treated with 10, 5, 2, and 0.5 μM concentrations of trifluoperazine were 8, 40, 68, and 80% transformed, respectively (Fig. 6). Parasites treated with trifluoperazine appeared morphologically and behaviorally similar to freshly hatched miracidia, indicating that this was not a phenotype of moribund or ''sick'' parasites.

Influence of SmCaM on sporocyst development: An RNA interference (RNAi) approach was used to evaluate the possible involvement of calmodulin on in vitro development of primary sporocysts. After 7 days of in vitro culture in the presence of double-stranded (ds) CaM RNA or control GFP dsRNA, parasites were examined to determine transcript abundance of both SmCaM1 and SmCaM2 transcripts via qPCR, protein levels of CaM with the use of Western blot, and physical phenotypes with the use of light microscopy. Moderate, but significant, reductions in transcript abundance levels were observed for both SmCaM1 and SmCaM2 (30 and 35%, respectively; $P \leq 0.05$) as a result of incubation in dsCaM RNA (Fig. 7A, B), as well as a concurrent reduction of 35% in total SmCaM protein levels with alpha-tubulin as a loading control (Fig. 7C). The only clearly defined morphological phenotype in the CaM dsRNA-treated parasites compared to the controls was an overall reduction in the length in CaM dsRNA-treated sporocysts (Fig. 8A), when compared to GFP dsRNA controls (Fig. 8B, C), $P \leq 0.05$ for

A

```
                              < EF-hand  >
SmCaM1      MADQLTEEQIAEFKEAFSLFDKDGDGTITTKELGTVMRSLGQNPTEAELQDMINEVD
FhCaM1      MADQLTEEQIAEFKEAFSLFDKDGDGTITTKELGTVMRSLGQNPTEAELQDMINEVD
 SjCaM      MADQLTEEQIAEFKEAFSLFDKDGDGTITTKELGTVMRSLGQNPTEAELQDMINEVD
 HsCaM      MADQLTEEQIAEFKEAFSLFDKDGDGTITTKELGTVMRSLGQNPTEAELQDMINEVD
DmCaMA      MADQLTEEQIAEFKEAFSLFDKDGDGTITTKELGTVMRSLGQNPTEAELQDMINEVD
 CeCaM      MADQLTEEQIAEFKEAFSLFDKDGDGTITTKELGTVMRSLGQNPTEAELQDMINEVD
 HcCaM      MADQLTEEQIAEFKEAFSLFDKDGDGTITTKELGTVMRSLGQNPTEAELQDMINEVD
SmCaM2      MADQLTEEQIAEFKEAFSLFDKDGDGTITTKELGTVMRSLGQNPTEAELQDMINEVD
            ------------------------------------------------------------

            < EF-hand  ><      Linker Helix    >< EF-hand  >
SmCaM1     ADGNGTIDFPEFLTMMARKMKDTDSEEEIREAFRVFDKDGNGFISAAELRHVMTNLGEKL
FhCaM1     ADGNGTIDFPEFLTMMARKMKDTDSEEEIREAFRVFDKDGNGFISAAELRHVMTNLGEKL
 SjCaM     ADGNGTIDFPEFLTMMARKMKDTDSEEEIREAFRVFDKDGNGFISAAELRHVMTNLGEKL
 HsCaM     ADGNGTIDFPEFLTMMARKMKDTDSEEEIREAFRVFDKDGNGYISAAELRHVMTNLGEKL
DmCaMA     ADGNGTIDFPEFLTMMARKMKDTDSEEEIREAFRVFDKDGNGFISAAELRHVMTNLGEKL
 CeCaM     ADGNGTIDFPEFLTMMARKMKDTDSEEEIREAFRVFDKDGNGFISAAELRHVMTNLGEKL
 HcCaM     ADGNGTIDFPEFLTMMARKMKDTDSEEEIREAFRVFDKDGNGFISAAELRHVMTNLGEKL
SmCaM2     ADGNGTIDFPEFLTMMARKMKDTDSEEEIREAFRVFDKDGNGFISAAELRHVMTNLGEKL
            ----------------------------------------*-------------------

                        < EF-hand  >
SmCaM1    TDDEVDEMIREADIDGDGQVNYEEFVKMMTAK
FhCaM1    TDEEVDEMIREADIDGDGQVNYEEFVKMMTAK
 SjCaM    TDEEVDEMIREADIDGDGQVNYEEFVKMMTAK
 HsCaM    TDEEVDEMIREADIDGDGQVNYEEFVQMMTAK
DmCaMA    TDEEVDEMIREADIDGDGQVNYEEFVTMMTSK
 CeCaM    TDEEVDEMIREADIDGDGQVNYEEFVTMMTTK
 HcCaM    TDEEVDEMIREADIDGDGQVNYEEFVTMMTTK
SmCaM2    TDDEVDEMIREADIDGDGQVNYEEFVTMMTTK
          --*------------------------*---*-
```

B

	SmCaM1	FhCaM1	SjCaM	HsCaM	DmCaMA	CeCaM	HcCaM	SmCaM2
SmCaM1		99	99	98	98	98	98	99
FhCaM1			100	99	99	99	99	98
SjCaM				99	99	99	99	98
HsCaM					98	98	98	97
DmCaMA						99	99	99
CeCaM							100	99
HcCaM								99

FIGURE 1. (**A**) Multiple amino acid sequence alignment of the 2 *Schistosoma mansoni* calmodulin proteins, SmCaM1 and SmCaM2, with other selected calmodulin proteins sharing high homology. Dashes (-) represent identical amino acid residues, and an asterisk (*) represents nonidentical amino acid residues. Brackets enclose the EF-hand domains (Ca-binding sites) and the alpha-helix linker domain acting as a flexible tether. Key: FhCaM, *Fasciola hepatica* (CAL91032); SjCaM, *Schistosoma japonicum* (AAW27335); HsCaM, *Homo sapiens* (NP_001734); DmCaMA, *Drosophila melanogaster* (NP_523710); CeCaM, *Caenorhabditis elegans* (NP_503386); HcCaM, *Haemonchus contortus* (CB012646). The alignments were prepared with the use of AlignX from the Vector NTI software package (Invitrogen). (**B**) Matrix showing percent identity shared between SmCaM1, SmCaM2, and other calmodulins.

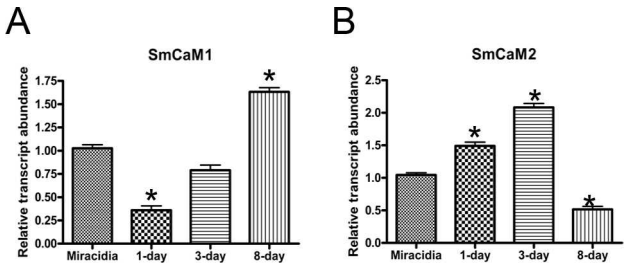

FIGURE 2. Relative transcript abundance of SmCaM1 (**A**) and SmCaM2 (**B**) during in vitro larval development of *Schistosoma mansoni* miracidia, and 1-, 3- and 8-day cultured sporocysts. Transcript levels were measured with the use of real-time quantitative PCR with GAPDH serving as a nonchanging template loading control. Columns represent average transcript abundance in sporocysts relative to miracidia. Error bars represent standard deviation for 3 separate biological replicates. $*P < 0.05$ relative to miracidia.

the 3 biological replicates. No discernible differences in SmCaM immunoreactivity patterns were noted in dsCaM-treated versus dsGFP-treated controls; nor were differences in CaM distribution observed between the ''long'' versus ''short'' sporocysts treated with CaM dsRNA (data not shown).

DISCUSSION

In the present study, we report the molecular cloning, expression analysis, and functional characterization of 2 calmodulin genes from *S. mansoni*. Although the presence of calmodulin protein(s) has been found during previous studies of *S. mansoni* adults, cercariae, and secreted in vitro transformation proteins of miracidia (Thompson et al., 1986; Siddiqui et al., 1991; Wu et al., 2009), there is very little information on the genes that encode these proteins or their functional significance in schistosome biology.

From EST data, we have found that the *S. mansoni* genome contains 2 calmodulin genes that appeared to encode separate transcripts. Further analysis of the genomic organization of these transcripts provides support that the 2 calmodulin transcripts are encoded by 2 distinct genes, rather than are the products of alternative splicing. If the 2 transcripts were derived from alternate splicing, our genomic PCR analysis would have indicated similar intron/exon boundaries, mutually exclusive exons, or alternative acceptor or donor sites. However, our data clearly indicate that SmCaM1 does indeed have the fourth intron in the location as predicted in the genome, whereas this intron in the same location is absent in the SmCaM2 gene. There is no indication, based on bioinformatic analysis, that the genes are located in proximity to each other, although this cannot be completely ruled out due to gaps in the genomic sequence data, and specifically, a gap of unknown length within 100 bp of the end of the SmCaM1 cDNA sequence. Other organisms have also been found to have multiple, identical calmodulin transcripts encoded by separate genes and not derived from alternative splicing. The protozoan parasite *Trypansosoma brucei rhodisiense* has 3 calmodulin genes arrayed in tandem, all with the same 5′ UTR (Tschudi and Ullu, 1988), while zebrafish have 3 identical, nonallelic calmodulin genes, all with significantly different 3′ UTRs (Friedberg and Rhoads, 2002). Mammals also have 3 nonidentical calmodulin genes on 3 separate chromosomes that encode identical proteins. However, these genes have differing 5′ and 3′ UTRs and promoter regions (Fischer et al., 1988; Nojima, 1989). To date, there are no genomic sequence data corresponding to SmCaM2, possibly due to the difficulty in assembling the sequences of these highly identical genes, or to the gaps or missing

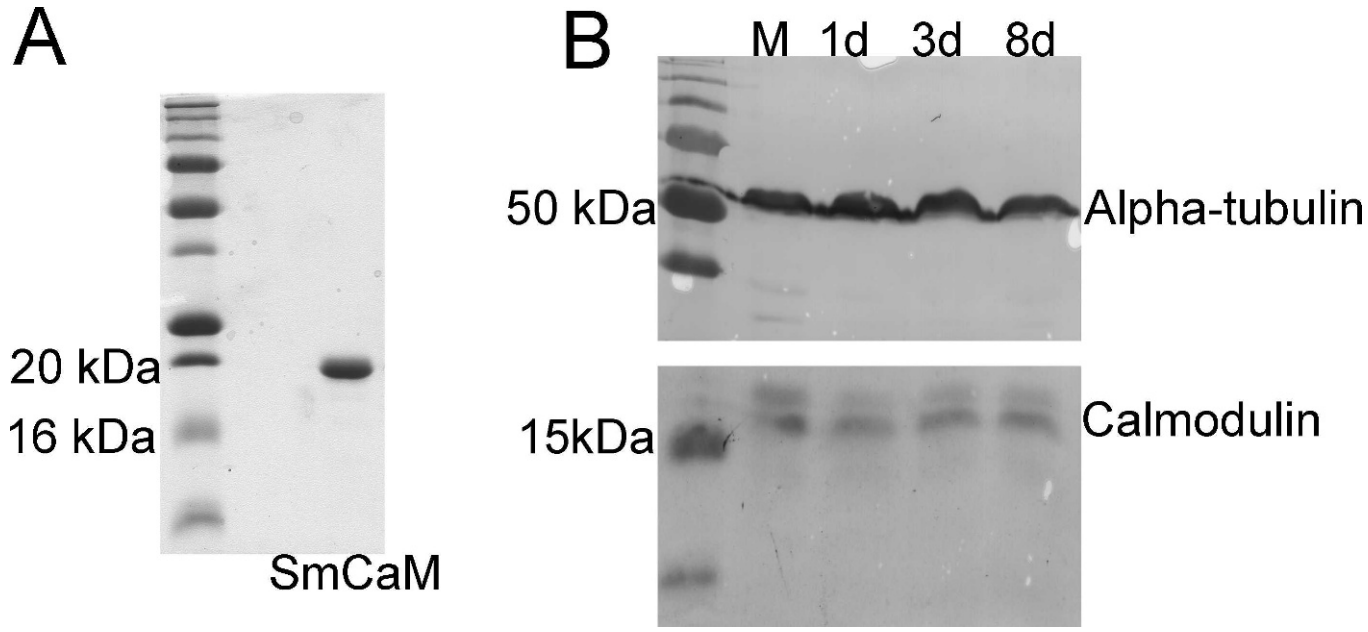

FIGURE 3. (**A**) Coomassie blue–stained SDS/PAGE gel of purified recombinant (r)SmCaM1 appearing as a single protein band at approximately 18 kDa. This was used for antibody production. (**B**) Western blot of protein expression levels for native *S. mansoni* calmodulin during larval development of miracidia and 1-, 3- or 8-day in vitro cultured sporocysts using an anti-rSmCaM1 antibody as probe. Anti-alpha tubulin was used as a control.

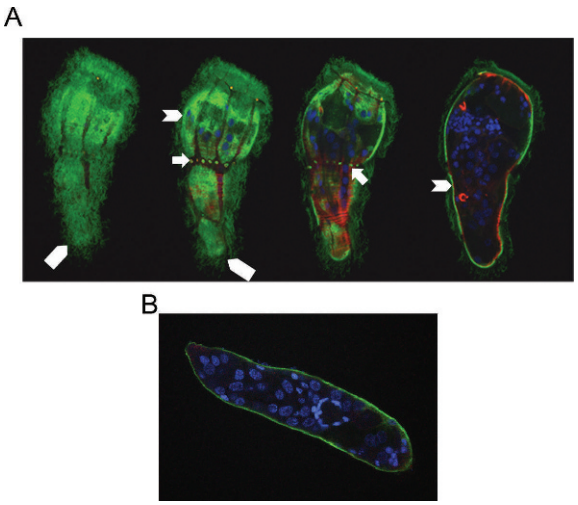

FIGURE 4. Confocal immunofluorescence microscopy of *Schistosoma mansoni* miracidia (**A**) and 3-day in vitro developing sporocysts (**B**). Miracidia and sporocysts were concurrently fixed and permeabilized and probed with anti-SmCaM. SmCaM reactivity was visualized using an Alexa Fluor®488-conjugated secondary antibody (green). Hoechst was used to visualize DNA/nuclei (blue), and phalloidin (red) was used to visualize actin-rich muscle tissue. In miracidia, arrows indicate nonciliated sensory papillae, chevrons indicate epidermal plates, and pentagons indicate cilia.

sequences in the newly reported *S. mansoni* genome (Berriman et al., 2009).

The 2 *S. mansoni* CaM transcripts exhibit differential transcript abundance patterns in miracidia and during early primary sporocyst development. SmCaM1 transcript abundance decreases in 1-day cultured sporocysts, relative to miracidia levels, then gradually increases in 3- and 8-day sporocysts, whereas SmCaM2 increases in 1- and 3-day sporocysts, compared to miracidia, then decreases in 8-day sporocysts to steady-state levels below miracidia. Currently, it is unknown whether these 2 genes, or their encoded proteins, are differentially regulated and expressed

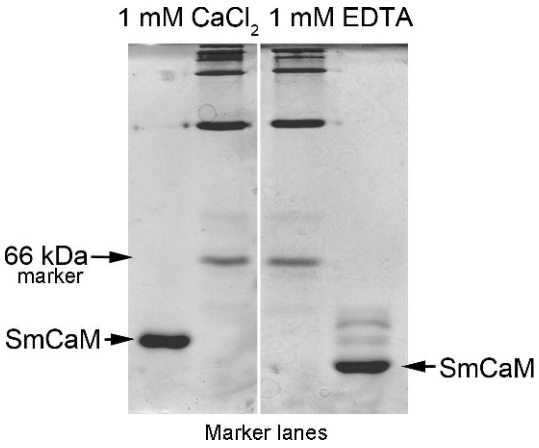

FIGURE 5. A nondenaturing PAGE gel demonstrating the calcium binding properties of SmCaM1. Recombinant SmCaM1 was run out on a nondenaturing PAGE gel containing 1 mM $CaCl_2$ or 1 mM EDTA in the resolving gel and the gel loading buffer and stained with Coomassie blue. Notice the reduced electrophoretic mobility of SmCaM when run on a PAGE gel containing 1 mM $CaCl_2$. The gels were aligned with NativeMark protein standards (Invitrogen).

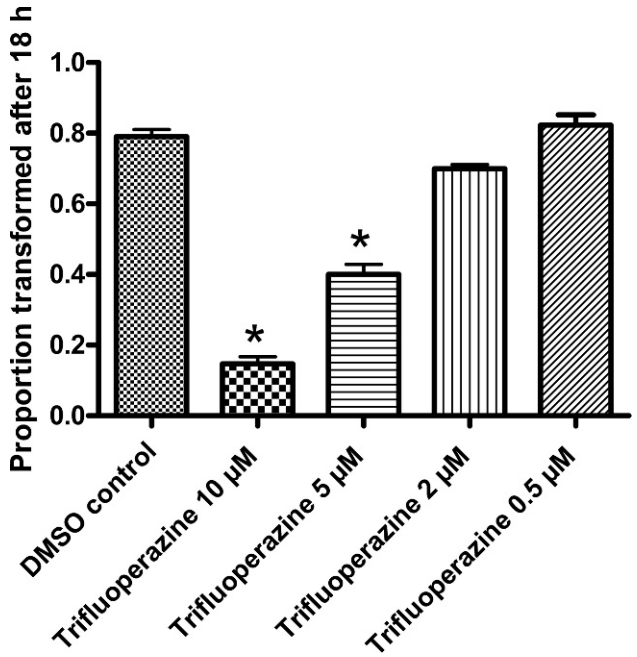

FIGURE 6. Effects of the CaM antagonist, trifluoperazine, on in vitro miracidium-to-sporocyst transformation in *Schistosoma mansoni*. Graph depicts a dose-dependent inhibition of miracidial transformation at 18 hr posttreated with 10, 5, 2, and 0.5 µM concentrations of trifluoperazine compared to the DMSO carrier-only control. * $P \leq 0.05$.

in dissimilar tissues, or if they have distinct functions. This remains a difficult question to answer because of the limited transgenic methodologies, e.g., gene transfer/expression techniques, or site-directed mutagenesis approaches, available for

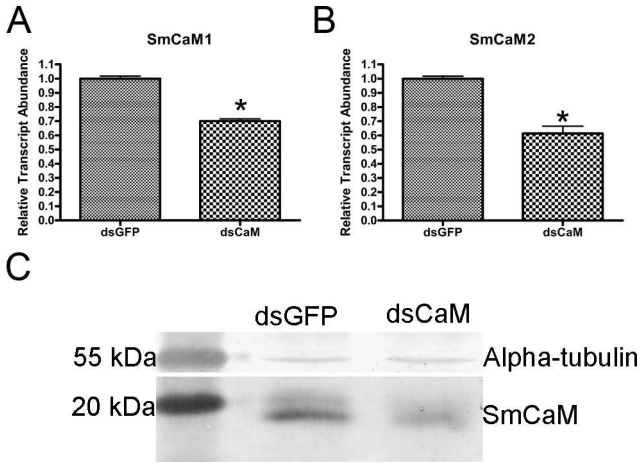

FIGURE 7. RNAi experiments in which *Schistosoma mansoni* larvae were treated with CaM dsRNA or control GFP dsRNA. Relative transcript abundance of SmCaM1 (**A**) and SmCaM2 (**B**) after 7 days of incubation in CaM dsRNA or control GFP dsRNA was determined by qPCR with GAPDH used as a constitutive template loading control. Transcript abundance levels for SmCaM1 and SmCaM2 dsRNA-treated sporocysts were decreased 30% and 35%, respectively, relative to control treatments. *$P < 0.05$. (**C**) Protein levels of SmCaM after treatment with CaM dsRNA compared to GFP dsRNA-treated parasites. Equal concentrations of total proteins were loaded per lane and confirmed with the use of alpha-tubulin as a protein loading control. Protein levels were quantified with the use of scanning densitometry. Notice reduced levels of SmCaM in the dsCaM-treated parasites.

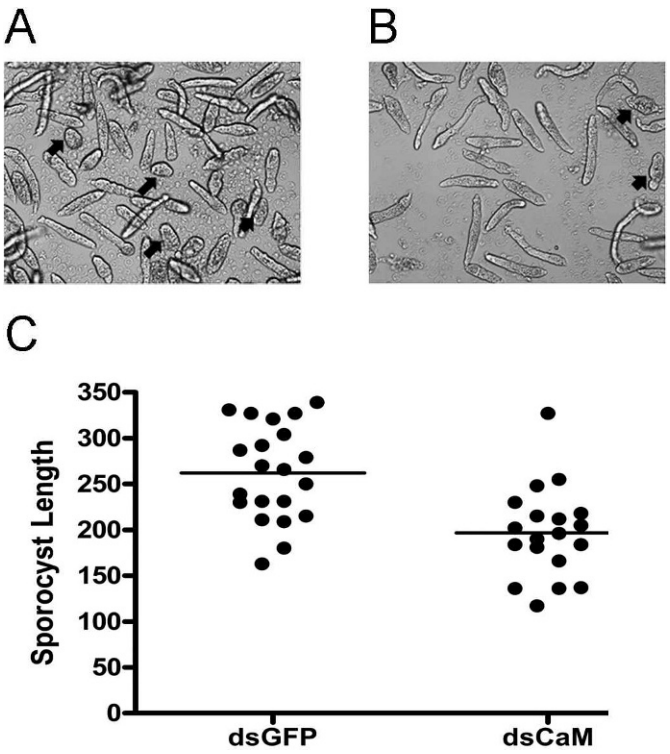

FIGURE 8. Brightfield images of CaM dsRNA-treated (**A**) and control GFP dsRNA-treated (**B**) *Schistosoma mansoni* sporocysts after 7 days of dsRNA exposure in complete medium. Note the reduced length, indicated with arrows, of more CaM dsRNA-treated sporocysts in comparison to control sporocysts. (**C**) Sporocyst length measurements are represented by scatter plots with the calculated median values indicated by the horizontal bars within each dsRNA treatment. The 2 treatments were statistically analyzed with the use of the Mann–Whitney *U*-test within each experiment, $P \leq 0.05$. This figure is representative of the 3 biological replicates.

functional genomic studies in schistosomes (Mann et al., 2010; Yoshino et al., 2010). The overall transcript abundance of both SmCaMs combined remains relatively unchanged during in vitro development, and this is reflected in similarities in CaM protein levels observed in miracidia and sporocysts during development. Western blot analysis of SmCaM levels in developing sporocysts demonstrates that CaM is a constitutively expressed protein. Because calmodulin is only active when bound to calcium, overall protein levels of CaM may not be indicative of a stage-specific importance of CaM, but rather its importance in regulating cellular function relating to calcium fluctuations during larval development.

Previously, Thompson et al. (1986) purified calmodulin from *S. mansoni* adults with the use of Ca^{2+}-dependent hydrophobic interaction chromatography and performed various functional studies with the use of the isolated protein. The purified calmodulin stimulated bovine heart adenosine 3′,5′-cyclic nucleotide phosphodiesterase (cAMP-specific PDE) in a Ca^{2+}-dependent manner, whereas calmodulin antagonists, commonly used as antipsychotics, e.g., calmidazolium, W-7, and trifluoperazine, inhibited the calmodulin-mediated activation of cAMP-specific PDE. In a previous study, Taft et al. (2010) found that the miracidium transformation process was regulated, in part, by cAMP signaling and that the incubation of miracidia in the phosphodiesterase (PDE) inhibitor isobutylmethylxanthine (IBMX) blocked transformation in a concentration-dependent manner. Additionally, it was found that IBMX treatment resulted in an increase in endogenous cAMP in treated miracidia. Thus, our finding that trifluoperazine (TFP) partially blocks transformation, combined with the previously reported findings that TFP inhibits cAMP-dependent PDE in adult worm extracts, strongly suggests that calmodulin likely plays a role in the regulation of the miracidium transformation process, possibly through the cAMP signaling pathway.

Our functional genomics studies of calmodulin using RNAi demonstrate that in vitro developing CaM ds-RNA treated sporocysts have reduced steady-state CaM transcript and protein abundance, and exhibit a concomitant reduction in average length as a result of CaM dsRNA treatment. Silencing the calmodulin gene (cmd-1) by RNAi in *C. elegans* also results in slowed growth (Kamath and Ahringer, 2003). This growth-retardation RNAi phenotype has been demonstrated with numerous *S. mansoni* transcripts in various stages, including a cathepsin B1 (SmCB1) in adult worms (Correnti et al., 2005), a CD36-type class B scavenger receptor (SRB) in sporocysts (Dinguirard and Yoshino, 2006), and Smad4, lactate dehydrogenase, Smad2, Cav2A, EF1α, Smad1, RHO2, calcineurin B, and ring box also in sporocysts (Mourao et al., 2009). This ''shortened'' phenotype appears to be the only visible morphological ''marker'' reported in dsRNA-treated sporocysts. It is plausible to assume that, because CaM is involved in so many diverse physiological processes (Van Eldik and Watterson, 1998), even a 35% knockdown in CaM protein levels may disrupt aspects of normal growth and development of the sporocyst. The knockdown of calmodulin transcripts in *S. mansoni* may have more dramatic effects on in vivo developing parasites in the snail host as ''normal'' larval development within the in vivo environment would require the full functioning of all regulatory networks, including CaM-involved pathways, for survival and development. Because our in vitro culture system provides only a rough approximation of the natural snail host, it may be hypothesized that the impact of specific gene knockdown would be manifested in a more general phenotype, such as slowed growth. This hypothesis is testable, because previous studies have shown that in vitro transformed primary sporocysts can be successfully transplanted into snails and remain viable (Granath and Yoshino, 1984; Kapp et al., 2003). However, to date, there have been no reports of dsRNA-treated sporocysts being implanted into snails.

Fluorescence confocal microscopy experiments clearly show that SmCaM is strongly associated with the cilia, epidermal plates, and nonciliated sensory papillae in miracidia and with the tegument of primary sporocysts. Our finding of CaM localized in the cilia is consistent with data identifying CaM as a component of ciliary and flagellar axonemes in various eukaryotic cells, including hamster tracheal epithelium, *Tetrahymena*, and *Chlamydamonas* (Gordon et al., 1982; Yang et al., 2001; Ueno et al., 2006). Calmodulin is primarily localized in the tegument of sporocysts that serves to transport solutes and nutrients into the parasite to be used for growth and development, as well as the exclusive host interface by which the parasite communicates with its external environment. Our finding that dsCaM-treated parasites are ''shortened'' compared to controls may indicate that the reduction in calmodulin may impair normal tegumental processes, possibly leading to decreased nutrient uptake leading to

a developmental delay or, because calmodulin has been implicated in muscle function in mammals (Walsh, 1994), another affected process associated with CaM dsRNA-treatment may be impairment of muscle function, leading to parasites with flaccid/rounded morphologies.

Both calcium ions and calmodulin have been identified as playing a role in egg hatching, and the presence of calmodulin has been demonstrated in mature and immature eggs during a large-scale proteomic study (Mathieson and Wilson, 2010). Calcium chelators, including EGTA, lanthanum chloride, and ruthenium red, also have been shown to inhibit egg hatching (Katsumata et al., 1989). This was shown not to be associated with toxicity, as the removal of these compounds allows eggs to hatch normally. Our finding that CaM is localized in sensory papillae may imply that SmCaM in these organs could be transducing calcium signals during the egg hatching process. CaM has been shown to be involved in sensory papillae function by regulating CaM-dependent phosphodiesterases (Borisy et al., 1993). Although we were able to reduce SmCaM transcript and protein levels with the use of RNAi in sporocysts, efforts to inhibit egg hatching using CaM dsRNA treatment of eggs were unsuccessful (data not shown).

In summary, we report the first in-depth characterization of calmodulin genes and their protein products in schistosomes. *Schistosoma mansoni* produces 2 nearly identical calmodulin transcripts encoded by separate genes, and although expression of the 2 transcripts varies during larval development, SmCaM protein levels remain the same in all larval stages tested. SmCaM protein was successfully expressed in *E. coli* and the purified recombinant protein exhibited functionality as a Ca ion-binding protein. Functional studies suggest a role of SmCaM during miracidium-to-sporocyst transformation (TFP inhibition) as well as its involvement in sporocyst larval development (RNAi studies). Finally, the tissue immunolocalization of CaM in miracidia corresponds to putative functions previously identified in other organisms using chemical calmodulin antagonists. In the future, the optimization of gene manipulation and transgenesis techniques in schistosomes may allow us to further characterize the role of the ubiquitous calcium signaling molecule, calmodulin.

ACKNOWLEDGMENTS

The authors would like to John Kunert for technical assistance in miracidia preparation and Lance Rodenkirch (W. M. Keck Laboratory for Biological Imaging, School of Medicine and Public Health, University of Wisconsin–Madison) for assistance with confocal microscopy. Fred Lewis (Biomedical Research Institute) provided schistosome-infected mice through NIH supply contract AI30026. This work was supported by NIH grant AI061436 to T.P.Y.

LITERATURE CITED

Berriman, M., B. J. Haas, P. T. LoVerde, R. A. Wilson, G. P. Dillon, G. C. Cerqueira, S. T. Mashiyama, B. Al-Lazikani, L. F. Andrade, P. D. Ashton et al. 2009. The genome of the blood fluke *Schistosoma mansoni*. Nature **460:** 352–358.

Borisy, F. F., P. N. Hwang, G. V. Ronnett, and S. H. Snyder. 1993. High-affinity cAMP phosphodiesterase and adenosine localized in sensory organs. Brain Research **610:** 199–207.

Chernin, E. 1963. Observations on hearts explanted in vitro from the snail *Australorbis glabratus*. Journal of Parasitology **49:** 353–364.

Cohen, P., and C. B. Klee. 1988. Calmodulin. Elsevier, New York, New York, 371 p.

Correnti, J. M., P. J. Brindley, and E. J. Pearce. 2005. Long-term suppression of cathepsin B levels by RNA interference retards schistosome growth. Molecular and Biochemical Parasitology **143:** 209–215.

Criscione, C. D., C. L. Valentim, H. Hirai, P. T. LoVerde, and T. J. Anderson. 2009. Genomic linkage map of the human blood fluke *Schistosoma mansoni*. Genome Biology **10:** R71.

Dinguirard, N., and T. P. Yoshino. 2006. Potential role of a CD36-like class B scavenger receptor in the binding of modified low-density lipoprotein (acLDL) to the tegumental surface of *Schistosoma mansoni* sporocysts. Molecular and Biochemical Parasitology **146:** 219–230.

Doenhoff, M. J., C. Donato, and J. Utzinger. 2008. Praziquantel: Mechanisms of action, resistance and new derivatives for schistosomiasis. Current Opinions in Infectious Diseases **21:** 659–667.

Dresden, M. H., and E. M. Edlin. 1974. *Schistosoma mansoni*: Effect of some cations on the proteolytic enzymes of cercariae. Experimental Parasitology **35:** 299–303.

Fischer, R., M. Koller, M. Flura, S. Mathews, M. A. Strehler-Page, J. Krebs, J. T. Penniston, E. Carafoli, and E. E. Strehler. 1988. Multiple divergent mRNAs code for a single human calmodulin. Journal of Biological Chemistry **263:** 17055–17062.

Fitzpatrick, J. M., E. Peak, S. Perally, I. W. Chalmers, J. Barrett, T. P. Yoshino, A. C. Ivens, and K. F. Hoffmann. 2009. Anti-schistosomal intervention targets identified by life cycle transcriptomic analyses. PLoS Neglected Tropical Diseases **3:** e543.

Friedberg, F., and A. R. Rhoads. 2002. Multiple calmodulin genes in fish. Molecular Biology Reports **29:** 377–382.

Fusco, A. C., B. Salafsky, G. Vanderkooi, and T. Shibuya. 1991. *Schistosoma mansoni*: The role of calcium in the stimulation of cercarial proteinase release. Journal of Parasitology **77:** 649–657.

Gordon, R. E., K. B. Williams, and S. Puszkin. 1982. Immune localization of calmodulin in the ciliated cells of hamster tracheal epithelium. Journal of Cell Biology **95:** 57–63.

Granath, W. O., Jr., and T. P. Yoshino. 1985. Surface antigens of *Biomphalaria glabrata* (Gastropoda) hemocytes: Functional heterogeneity in cell subpopulations recognized by a monoclonal antibody. Journal of Invertebrate Pathology **45:** 174–186.

Hansen, E. L., G. Perez-Mendez, and E. Yarwood. 1974. *Schistosoma mansoni*: Axenic culture of daughter sporocysts. Experimental Parasitology **36:** 40–44.

Havercroft, J. C., M. C. Huggins, D. W. Dunne, and D.W. Taylor. 1990. Characterisation of Sm20, a 20-kilodalton calcium-binding protein of *Schistosoma mansoni*. Molecular and Biochemical Parasitology **38:** 211–219.

Hu, S., P. Law, Z. Lu, Z. Wu, and M. C. Fung. 2008. Molecular characterization of a calcium-binding protein SjCa8 from *Schistosoma japonicum*. Parasitology Research **103:** 1047–1053.

Ikeda, T. 2001. Effect of ionophores on in vitro excystment of *Paragonimus ohirai* metacercariae. Parasitology Research **87:** 343–344.

———. 2004. Effects of blockers of Ca2+ channels and other ion channels on in vitro excystment of *Paragonimus ohirai* metacercariae induced by sodium cholate. Parasitology Research **94:** 329–331.

———. 2006. Effects of L-type Ca2+ channel antagonists on in vitro excystment of *Paragonimus ohirai* metacercariae induced by sodium cholate. Parasitology Research **99:** 336–340.

Jolly, E. R., C. S. Chin, S. Miller, M. M. Bahgat, K. C. Lim, J. DeRisi, and J. H. McKerrow. 2007. Gene expression patterns during adaptation of a helminth parasite to different environmental niches. Genome Biology **8:** R65.

Kamath, R. S., and J. Ahringer. 2003. Genome-wide RNAi screening in *Caenorhabditis elegans*. Methods **30:** 313–321.

Kapp, K., C. Coustau, V. Wippersteg, J. Jourdane, W. Kunz, and C. G. Grevelding. 2003. Transplantation of in vitro-generated *Schistosoma mansoni* mother sporocysts into *Biomphalaria glabrata*. Parasitology Research **91:** 482–485.

Katsumata, T., S. Kohno, K. Yamaguchi, K. Hara, and Y. Aoki. 1989. Hatching of *Schistosoma mansoni* eggs is a Ca2+/calmodulin-dependent process. Parasitology Research **76:** 90–91.

———, M. Shimada, K. Sato, and Y. Aoki. 1988. Possible involvement of calcium ions in the hatching of *Schistosoma mansoni* eggs in water. Journal of Parasitology **74:** 1040–1041.

KAWAMOTO, F., A. SHOZAWA, N. KUMADA, AND K. KOJIMA. 1989. Possible roles of cAMP and Ca2+ in the regulation of miracidial transformation in *Schistosoma mansoni*. Parasitology Research **75:** 368–374.

KING, C. H. 2007. Lifting the burden of schistosomiasis—Defining elements of infection-associated disease and the benefits of antiparasite treatment. Journal of Infectious Diseases **196:** 653–655.

KNUDSEN, G. M., K. F. MEDZIHRADSZKY, K. C. LIM, E. HANSELL, AND J. H. MCKERROW. 2005. Proteomic analysis of *Schistosoma mansoni* cercarial secretions. Molecular and Cellular Proteomics **4:** 1862–1875.

LEWERT, R. M., D. R. HOPKINS, AND S. MANDLOWITZ. 1966. The role of calcium and magnesium ions in invasiveness of schistosome cercariae. American Journal of Tropical Medicine and Hygiene **15:** 314–323.

LIVAK, K. J., AND T. D. SCHMITTGEN. 2001. Analysis of relative gene expression data using real-time quantitative PCR and the 2(-Delta Delta C(T)) method. Methods **25:** 402–408.

MANN, V. H., M. E. MORALES, G. RINALDI, AND P. J. BRINDLEY. 2010. Culture for genetic manipulation of developmental stages of *Schistosoma mansoni.* Parasitology **137:** 451–462.

MATHIESON, W., AND R. A. WILSON. 2010. A comparative proteomic study of the undeveloped and developed *Schistosoma mansoni* egg and its contents: The miracidium, hatch fluid and secretions. International Journal for Parasitology **40:** 617–628.

MELMAN, S. D., M. L. STEINAUER, C. CUNNINGHAM, L. S. KUBATKO, I. N. MWANGI, N. B. WYNN, M. W. MUTUKU, D. M. KARANJA, D. G. COLLEY, C. L. BLACK ET AL. 2009. Reduced susceptibility to praziquantel among naturally occurring Kenyan isolates of *Schistosoma mansoni*. PLoS Neglected Tropical Diseases **3:** e504.

MOSER, D., M. J. DOENHOFF, AND M. Q. KLINKERT. 1992. A stage-specific calcium-binding protein expressed in eggs of *Schistosoma mansoni*. Molecular and Biochemical Parasitology **51:** 229–238.

MOURAO, M. M., N. DINGUIRARD, G. R. FRANCO, AND T. P. YOSHINO. 2009. Phenotypic screen of early-developing larvae of the blood fluke, *Schistosoma mansoni*, using RNA interference. PLoS Neglected Tropical Diseases **3:** e502.

NOJIMA, H. 1989. Structural organization of multiple rat calmodulin genes. Journal of Molecular Biology **208:** 269–282.

NOLAN, L. E., AND M. R. CARRIKER. 1946. Observations on the biology of the snail *Lymnaea stagnalis appressa* during twenty years in laboratory culture. American Midland Naturalist **36:** 467–493.

SALATHE, M. 2007. Regulation of mammalian ciliary beating. Annual Review of Physiology **69:** 401–422.

SAMBROOK, J., E. F. FRITSCH, AND T. MANIATIS. 1989. Molecular cloning: A laboratory manual, 2nd ed. Cold Spring Harbor Laboratory Press, Plainview, New York, 1639 p.

SHEN, X., C. A. VALENCIA, W. GAO, S. W. COTTEN, B. DONG, B. C. HUANG, AND R. LIU. 2008. Ca(2+)/calmodulin-binding proteins from the *C. elegans* proteome. Cell Calcium **43:** 444–456.

SHETERLINE, P. 1980. Trifluoperazine can distinguish between myosin light chain kinase and troponin C-linked control of actomyosin interaction by Ca++. Biochemical and Biophysical Research Communications **93:** 197–208.

SIDDIQUI, A. A., R. B. PODESTA, AND M. W. CLARKE. 1991. *Schistosoma mansoni*: Characterization and identification of calcium-binding proteins associated with the apical plasma membrane and envelope. Experimental Parasitology **72:** 63–68.

STEINMANN, P., J. KEISER, R. BOS, M. TANNER, AND J. UTZINGER. 2006. Schistosomiasis and water resources development: Systemic review, meta analysis, and estimates of people at risk. Lancet—Infectious Diseases **6:** 411–425.

TAFT, A. S., F. A. NORANTE, AND T. P. YOSHINO. 2010. The identification of inhibitors of *Schistosoma mansoni* miracidial transformation by incorporating a medium-throughput small-molecule screen. Experimental Parasitology **125:** 84–94.

———, J. J. VERMEIRE, J. BERNIER, S. R. BIRKELAND, M. J. CIPRIANO, A. R. PAPA, A. G. MCARTHUR, AND T.P. YOSHINO. 2009. Transcriptome analysis of *Schistosoma mansoni* larval development using serial analysis of gene expression (SAGE). Parasitology **136:** 469–485.

THOMPSON, D. P., G. Z. CHEN, A. K. SAMPLE, D. R. SEMEYN, AND J. L. BENNETT. 1986. Calmodulin: Biochemical, physiological, and morphological effects on *Schistosoma mansoni*. American Journal of Physiology **251:** R1051–R1058.

TSCHUDI, C., AND E. ULLU. 1988. Polygene transcripts are precursors to calmodulin mRNAs in trypanosomes. EMBO Journal **7:** 455–463.

UENO, H., Y. IWATAKI, AND O. NUMATA. 2006. Homologues of radial spoke head proteins interact with Ca2+/calmodulin in *Tetrahymena* cilia. Journal of Biochemistry **140:** 525–533.

VAN ELDIK, L. J., AND D. M. WATTERSON. 1998. Calmodulin and signal transduction, 1st ed. Academic Press, Maryland Heights, Missouri, 482 p.

VERMEIRE, J. J., A. S. TAFT, K. F. HOFFMANN, J. M. FITZPATRICK, AND T.P. YOSHINO. 2006. *Schistosoma mansoni*: DNA microarray gene expression profiling during the miracidium-to-mother sporocyst transformation. Molecular and Biochemical Parasitology **147:** 39–47.

WALSH, M. P. 1994. Calmodulin and the regulation of smooth muscle contraction. Molecular and Cellular Biochemistry **135:** 21–41.

WU, X. J., G. SABAT, J. F. BROWN, M. ZHANG, A. TAFT, N. PETERSON, A. HARMS, AND T. P. YOSHINO. 2009. Proteomic analysis of *Schistosoma mansoni* proteins released during in vitro miracidium-to-sporocyst transformation. Molecular and Biochemical Parasitology **164:** 32–44.

YANG, P., D. R. DIENER, J. L. ROSENBAUM, AND W. S. SALE. 2001. Localization of calmodulin and dynein light chain LC8 in flagellar radial spokes. Journal of Cell Biology **153:** 1315–1326.

YOSHINO, T. P. 1981. Comparison of concanavalin A–reactive determinants on hemocytes of two *Biomphalaria glabrata* snail stocks: Receptor binding and redistribution. Developmental and Comparative Immunology **5:** 229–240.

———, N. DINGUIRARD, AND M. M. MOURAO. 2010. *In vitro* manipulation of gene expression in larval *Schistosoma*: A model for postgenomic approaches in Trematoda. Parasitology **137:** 463–483.

———, AND J. R. LAURSEN. 1995. Production of *Schistosoma mansoni* daughter sporocysts from mother sporocysts maintained in synxenic culture with *Biomphalaria glabrata* embryonic (Bge) cells. Journal of Parasitology **81:** 714–722.

ZERLOTINI, A., M. HEIGES, H. WANG, R. L. MORAES, A. J. DOMINTINI, J. C. RUIZ, J. C. KISSINGER, AND G. OLIVEIRA. 2009. SchistoDB: A *Schistosoma mansoni* genome resource. Nucleic Acids Research **37:** 579–582.